Supplement of Atmos. Chem. Phys., 25, 6395–6406, 2025
https://doi.org/10.5194/acp-25-6395-2025-supplement
© Author(s) 2025. CC BY 4.0 License.

Atmospheric Chemistry and Physics
Open Access

Supplement of

Direct measurement of N_2O_5 heterogeneous uptake coefficients on atmospheric aerosols in southwestern China and evaluation of current parameterizations

Jiayin Li et al.

Correspondence to: Xiaorui Chen (chenxr95@mail.sysu.edu.cn) and Keding Lu (k.lu@pku.edu.cn)

The copyright of individual parts of the supplement might differ from the article licence.

Contents

S1. Detailed description of the measurement and calculation of $\gamma(N_2O_5)$.

S2. Calculate of organic wet mass fraction.

Figure S1. Overall schematic of aerosol flow tube system. Bold arrows indicate the main lines of the sampling gas.

Figure S2. Time series of measured concentrations of NO_2, O_3, NO, $PM_{2.5}$ and N_2O_5, the values of $\gamma(N_2O_5)$, and meteorological parameters of RH and T during the campaign.

Figure S3. NO_3 reactivity with VOCs.

Figure S4. Time series of N_2O_5 and NO_3 lifetime during the campaign.

Figure S5. The distribution of parameterized $\gamma(N_2O_5)$ values of GRI09 (a) and BT09 (b).

Table S1. Summary of field observation results of nocturnal NO_3 and N_2O_5 concentrations, $P(NO_3)$, and $\tau(N_2O_5)$ from various regions around the world in recent years.

Table S2. Summary of global field observation results of $\gamma(N_2O_5)$.

Table S3. Pearson Correlation Coefficient (r) among factors affecting $\gamma(N_2O_5)$.

Table S4. Summary of the details and performances of the parameterizations discussed in this study.

S1. Detailed description of the measurement and calculation of $\gamma(N_2O_5)$

The Aerosol Flow Tube System (AFTS) can be divided into three main modules: the sampling control module, the reaction module, and the detection module. The sampling of the flow tube is facilitated by a vacuum pump located at the end of the system. In the sampling control module, ambient air is directly introduced into the reaction pathway. The sampling gas passes through a 1-in/2-out solenoid valve that directs the sample either through a HEPA filter to remove aerosols or bypasses it, thereby controlling the presence of aerosols in the reaction module. The sampling gas is then mixed with a high concentration of N_2O_5 generated from a N_2O_5 source before entering the reaction module. At the top of the reaction module, two stainless steel static mixers are installed to ensure that the gas is thoroughly mixed. The aerosol flow tube is the primary site for N_2O_5 uptake reactions.

During detection, concentrations of NO_x and O_3 are continuously measured at the top of the flow tube to facilitate subsequent simulation of gas-phase reactions within the flow tube using a box model. The measurement of N_2O_5 concentration is conducted through two separate 20-minute processes: one to determine the N_2O_5 loss rate in the absence of aerosols (k_{wall}) and another in the presence of aerosols ($k_{wall}+k_{aerosol}$). The only difference between the two processes is the presence or absence of aerosols. Each process includes two steps: measuring N_2O_5 concentrations at both the top and bottom of the flow tube, each step maintains 10 min. Throughout the measurement process, the aerosol surface area (Sa) is continuously measured at the bottom of the flow tube, followed by size-resolved Sa correction based on previously determined particle loss coefficients(Chen et al., 2022).

By inputting the measured concentrations of NO_x, O_3, and N_2O_5 at the top of the flow tube under both aerosol-free and aerosol-present conditions into the box model, the NO_3-N_2O_5 chemical reactions and related gas-phase reactions in the flow tube are simulated until the model's output N_2O_5 concentration matches the measured value at the tube's bottom. This process yields k_{wall} and $k_{wall}+k_{aerosol}$, from which the N_2O_5 loss rate on aerosols ($k_{aerosol}$) is derived by subtraction. The $\gamma(N_2O_5)$ can then be calculated using established formulas (EqS1).

$$k_{N2O5} = 0.25 \times Sa \times \gamma \times C \qquad \text{（EqS1）}$$

The uncertainty in $\gamma(N_2O_5)$ is relevant to the measurement uncertainties of each instrument and the rapid fluctuations of various parameters. To ensure accurate measurements, a rigorous data screening process was implemented. A 10% cutoff for

N_2O_5 variation was applied to exclude air masses that were too unstable for valid analysis according to our data screening criteria. Cases showing more than a 2% variation in relative humidity (RH) between HEPA inline and bypass modes were excluded due to RH's significant influence on k_{wall} of N_2O_5 in the aerosol flow tube. To ensure significant N_2O_5 concentration differences due to heterogeneous uptake reactions between the top and bottom of the flow tube, periods with low Sa conditions (<100 μm^2 cm^{-3}) were filtered out. Additionally, cases where NO concentration exceeded 7 ppbv were excluded to avoid significant changes in NO_3-N_2O_5 concentration due to NO titration in the flow tube.

Therefore, the system may introduce a 2% measurement bias in $\gamma(N_2O_5)$ due to N_2O_5 concentration fluctuations, a bias of $\pm 8\times10^{-4}$ to $\pm 2\times10^{-3}$ due to RH fluctuations, a 16% uncertainty from Sa measurement and particle loss in the flow tube, a 4% measurement fluctuation from Monte Carlo simulations, up to a 9% uncertainty from ambient temperature variations, and a 5% uncertainty from NO_x and O_3 concentration fluctuations. In summary, considering all the factors and their corresponding varying ranges discussed above, the overall uncertainty of $\gamma(N_2O_5)$ determined from Monte Carlo simulations ranges from 16% to 43%.

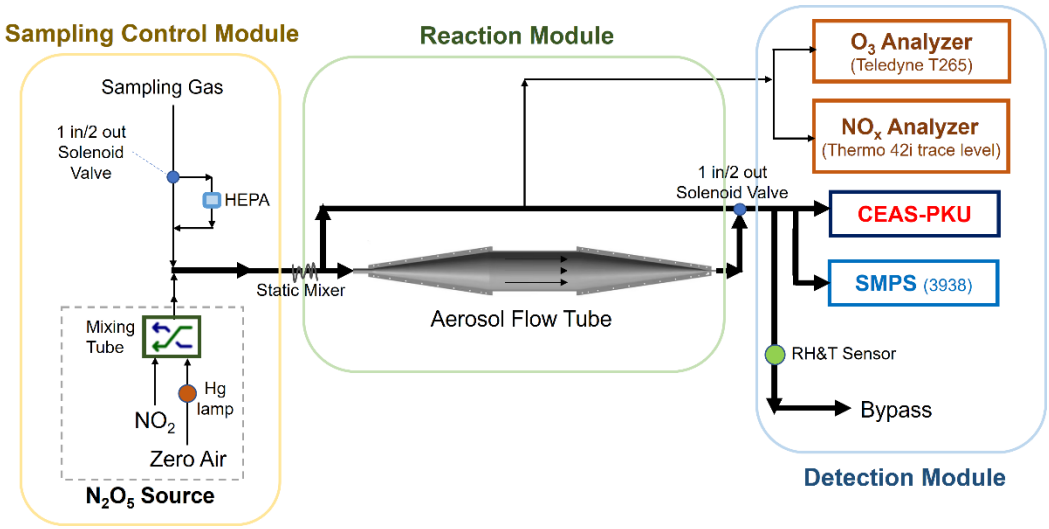

Figure S1. Overall schematic of aerosol flow tube system. Bold arrows indicate the main lines of the sampling gas.

S2. Calculate of organic wet mass fraction.

The organic wet mass fraction is defined as the mass fraction of organics within the aerosol containing water. The calculation of organic wet mass fraction is presented as follows.

$$\text{Organic wet mass fraction}=\text{Organic mass}/(\text{Organic mass}+NO_3^- \text{ mass}+Cl^- \text{ mass}+SO_4^{2-} \text{ mass}+NH_4^+ \text{ mass}+H_2O \text{ mass})$$

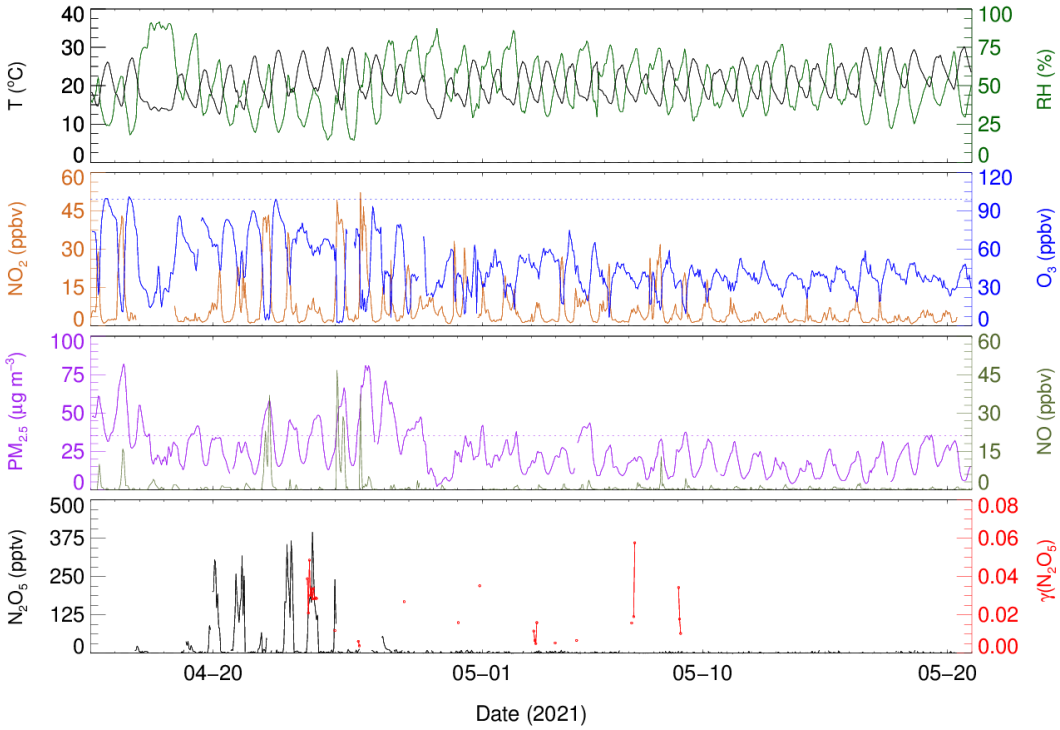

Figure S2. Time series of measured concentrations of NO_2, O_3, NO, $PM_{2.5}$ and N_2O_5, the values of $\gamma(N_2O_5)$, and meteorological parameters of RH and T during the campaign. The blue line and the purple line represent Chinese national air quality standards for O_3 and $PM_{2.5}$, respectively.

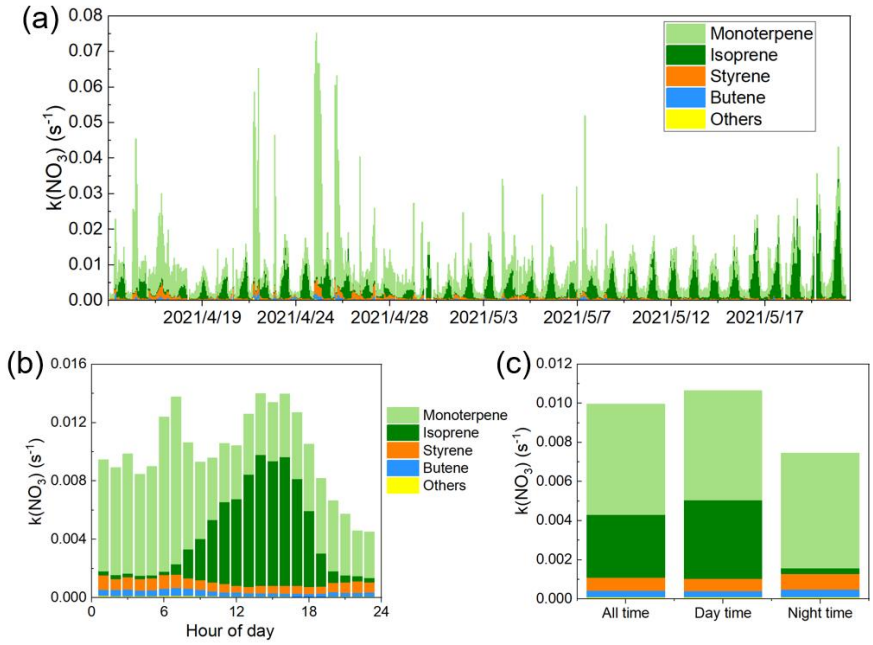

Figure S3. NO_3 reactivity with VOCs. (a) Time series of VOCs contributions for $k(NO_3)$. (b) Mean diurnal profiles of $k(NO_3)$. (c) The contribution of VOCs categories for $k(NO_3)$.

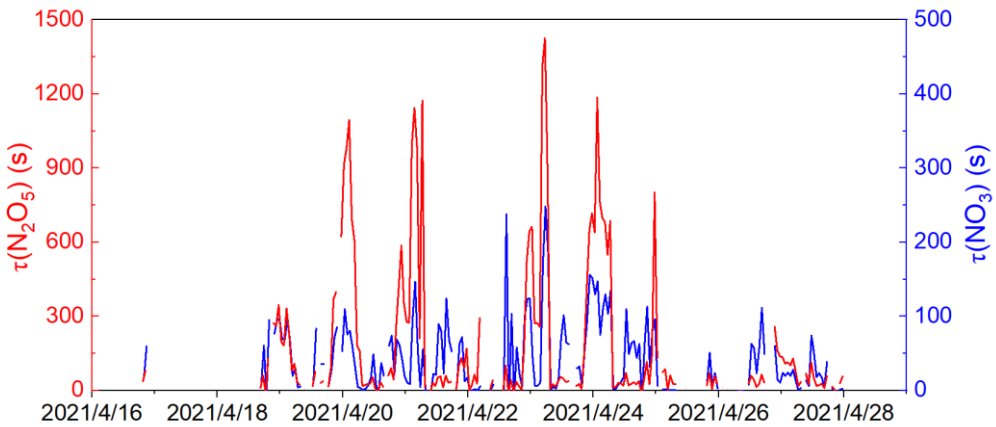

Figure S4. Time series of N_2O_5 and NO_3 lifetime during the campaign.

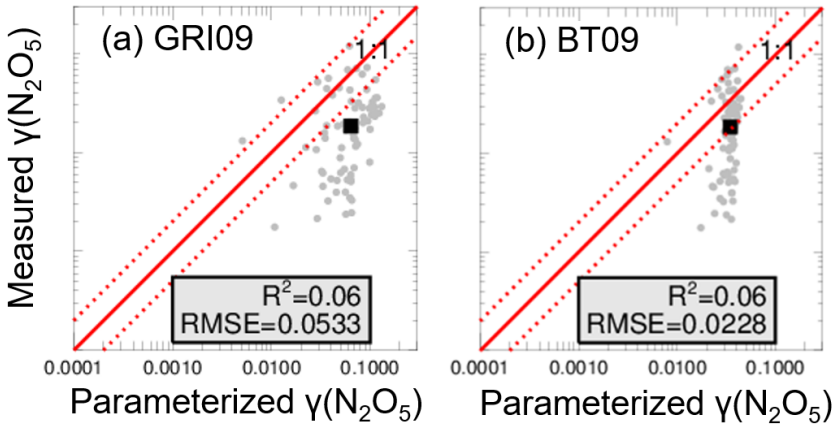

Figure S5. The distribution of parameterized $\gamma(N_2O_5)$ values of GRI09 (a) and BT09 (b).

Table S1. Summary of field observation results of nocturnal NO_3 and N_2O_5 concentrations, $P(NO_3)$, and $\tau(N_2O_5)$ from various regions around the world in recent years.

Location	Site type	Period	NO_3 (pptv) (night)	N_2O_5 (pptv) (night)	$P(NO_3)$ (ppbv/h)	$\tau(N_2O_5)$ (s)	Reference
Kunming, China	Suburban	2021.04	5.7±3.2	33.4±75.2 (395.1)	0.6± 0.1	185±294	This work
Beijing, China	Rural	2016.05	27	73±90 (937)	1.2 ± 0.9	270±240	(Wang et al., 2018)
Bejing, China	Urban	2016.09	-	36.7	1.4 ± 1.7	-	(Wang et al., 2017a)
Bejing, China	Suburban	2016.02	-	~1400	-	-	(Wang et al., 2020b)
Wangdu, China	Rural	2014.07	-	~200 (430)	1.7±0.6	76.9	(Tham et al., 2016)
Mountain Tai, China	Suburban	2014.07	-	6.8±7.7	0.5±0.4	74	(Wang et al., 2017c)
Jinan, China	Urban	2014.08	-	22±12 (278)	-	-	(Wang et al., 2017b)
Shanghai, China	Urban	2011.08	16±9	310±380	1.1±1.1	-	(Wang et al., 2013)
Taizhou, China	Rural	2018.05	4.4±2.2	26.0±35.7 (492)	1.0×0.5	43 ± 52	(Wang et al., 2020a)
Taizhou, China	Suburban	2018.05	4.4±2.2	26.0 ± 35.7	1.2±0.4	55±68	(Li et al., 2020)
Changzhou, China	Suburban	2019.05	-	61.0 ± 63.1 (477.2)	2.8 ± 1.6	-	(Zhai et al., 2023)

Hongkong, China	Island	2012.08	7 ±12	17±33 (336)	-	76±61	(Yan et al., 2019)
Hongkong, China	Coastal	2013.11	-	~11800	0.26	~13 h	(Brown et al., 2016)
Shenzhen, China	Coastal	2019.09	-	56±89 (1420)	2.9±0.5	-	(Niu et al., 2022)
Heshan, China	Urban	2019.09	~90	64±145	2.5±2.1	-	(Wang et al., 2022)
South China Sea	Island	2021.11	10 ±13	120±129	1.4±0.7	30±42	(Wang et al., 2024)
Seoul, Korea	Urban, tower	2015.05	-	4100±1200, 2600±1600 (5000)	1.3	1800	(Brown et al., 2017)
Southern Spain	Coastal	2008.11	-	~500	-	-	(Crowley et al., 2011)
Northwestern, Europe	Coastal, airborne	2010.07	-	670	-	15~120 min	(Morgan et al., 2015)
Taunus Observatory, Germany	Rural	2011.08	-	~800	~1.8	-	(Phillips et al., 2016)
East coast USA	Coastal	2002.06	17	84	-	-	(Brown et al., 2004)
California, USA	Coastal	2004.01	-	~200	-	~30 min	(Wood et al., 2005)
Salt Lake Valley, USA	Airborne	2017.01	-	0~2	0~2	-	(McDuffie et al., 2019)
Lower Fraser Valley, Canada	Suburban	2012.07	-	1.4 (23)	-	-	(Osthoff et al., 2018)

The values in brackets are the maximum of N_2O_5 concentration.

Table S2. Summary of global field observation results of $\gamma(N_2O_5)$.

Location	Period	Site type	$\gamma(N_2O_5)$	Method	Reference
Kunming, China	2021.04	Suburban	0.0018~0.12 (0.23±0.21)	AFTS	This work
Beijing, China	2016.02	Suburban	0.001-0.02 (0.0046)	Box model	(Wang et al., 2020b)
Beijing, China	2016.05	Rural	0.012-0.055 (0.034)	Products	(Wang et al., 2018)
Beijing, China	2016.09	Urban	0.025-0.072 (0.048)	Steady-state	(Wang et al., 2017a)
Beijing, China	2018.1	Urban	0.0075-0.0149	Steady-state	(Xia et al., 2021)
Beijing, China	2019.01	Tower	0.0005-0.2 (0.05)	Box model	(Chen et al., 2020)
Beijing, China	2020.12	Urban	0.0045-0.12 (0.042±0.026)	AFTS	(Chen et al., 2022)
Wangdu, China	2014.06	Rural	0.005-0.039	Products	(Tham et al., 2018)
Wangdu, China	2014.06	Rural	0.0012-0.072	Steady-state	(Lu et al., 2022)
Wangdu, China	2017.12	Rural	0.006-0.015	Steady-state	(Xia et al., 2021)
Mountain Tai, China	2014.07	Suburban	0.021-0.102 (0.061)	Steady-state	(Wang et al., 2017c)
Mountain Tai, China	2018.03	Suburban	0.001-0.019 (0.01)	AFTS	(Yu et al., 2020)
Jinan, China	2014.08	Urban	0.042-0.092 (0.069)	Steady-state	(Wang et al., 2017b)
Taizhou, China	2018.06	Suburban	0.027-0.107 (0.08)	Steady-state	(Li et al., 2020)
Changzhou, China	2019.06	Suburban	0.057-0.123 0.001-0.024	Steady-state Parameterization	(Zhai et al., 2023)
Hongkong, China	2013.11	Suburban	0.004-0.029 (0.014)	Steady-state	(Brown et al., 2016)
Hongkong, China	2013.11	Suburban	0.0005-0.016 (0.004)	Box model	(Yun et al., 2018)
Heshan, China	2017.03	Suburban	0.002-0.067 (0.02)	AFTS	(Yu et al., 2020)
Heshan, China	2019.10	Urban	0.0019-0.077 (0.0317)	Products	(Wang et al., 2022)
Shenzhen, China	2019.10	Coastal	0.002-0.068 (0.027±0.02)	Products	(Niu et al., 2022)

Location	Period	Site type	$\gamma(N_2O_5)$	Method	Reference
			0.005-0.08 (0.031±0.02)	Box model	
New England, USA	2002.08	Ship	0.03-0.04	Steady-state	(Aldener et al., 2006)
New England, USA	2004.02	Airborne	0.0016-0.02	Steady-state	(Brown et al., 2006)
Texas, USA	2006.10	Airborne	0.0005-0.006 (0.0039)	Steady-state	(Brown et al., 2009)
Boulder, USA	2008.07	Tower	0.0009-0.012 (0.003)	AFTS	(Bertram et al., 2009)
Seattle, USA	2008.08	Coastal	0.005-0.04	AFTS	(Bertram et al., 2009)
California, USA	2009.09	Coastal	0.00003-0.029 (0.0054)	AFTS	(Riedel et al., 2012)
Los Angeles, USA	2010.05	Airborne	0.001-0.01	Steady-state	(Chang et al., 2016)
Colorade, USA	2011.02	Tower	0.002-0.1 (0.04)	Box model	(Wagner et al., 2013)
Eastern，USA	2015.02	Airborne	0.00002-0.175 (0.014)	Box model	(McDuffie et al., 2018)
Salt Lake Valley, USA	2017.01	Airborne	0.001-0.1 (0.076)	Box model	(McDuffie et al., 2019)
NW Europe/UK	2010.06	Airborne	0.0076-0.03	Steady-state	(Morgan et al., 2015)
SW Germany	2011.08	Suburban	0.004-0.11 (0.028)	Products, Steady-state	(Phillips et al., 2016)

The values in brackets are mean values of $\gamma(N_2O_5)$.
AFTS: aerosol flow tube system;
Steady-state: steady state approximation;
Products: products formation rate analysis;
Box model: inverse iterative box model simulation.

Table S3. Pearson Correlation Coefficient (r) among factors affecting $\gamma(N_2O_5)$, the statistical data are limited to the period in which measured $\gamma(N_2O_5)$ is available.

Factors	Temp	RH	Aerosol Water	Aerosol Nitrate	H_2O/NO_3^- Molar ratio	Aerosol Chloride	Cl^-/NO_3^- Molar ratio	Org dry mass fraction	Org wet mass fraction	Org/SO_4^{2-}
Temp	1.00	-0.85	-0.45	-0.27	0.09	-0.30	-0.12	0.15	0.24	0.09
RH	-	1.00	0.49	0.45	-0.27	0.24	-0.09	-0.12	-0.23	-0.08
Aerosol Water	-	-	1.00	-0.40	0.62	-0.10	0.19	-0.66	-0.79	-0.68
Aerosol Nitrate	-	-	-	1.00	-0.80	0.24	-0.39	0.34	0.38	0.43
H_2O/NO_3^- Molar ratio	-	-	-	-	1.00	-0.21	0.45	-0.64	-0.67	-0.67
Aerosol Chloride	-	-	-	-	-	1.00	0.69	-0.02	0.01	0.06
Cl^-/NO_3^- Molar ratio	-	-	-	-	-	-	1.00	-0.37	-0.35	-0.33
Org dry mass fraction	-	-	-	-	-	-	-	1.00	0.98	0.97
Org wet mass fraction	-	-	-	-	-	-	-	-	1.00	0.96
Org/SO_4^{2-}	-	-	-	-	-	-	-	-	-	1.00

Table S4. Summary of the details and performances of the parameterizations discussed in this study.

Parameterization name	Factors considered	Parameterization	Reference	R^2	RMSE	Median
RIE03	Mass concentration of aerosol sulfate and nitrate ($\mu g/m^3$)	$\boldsymbol{\gamma = f \times r_1 + (1-f) \times r_2}$ where, $r_1=0.02$ $r_1=0.002$ f= mass SO_4^{2-}/(mass SO_4^{2-}+ mass NO_3^-)	(Riemer et al., 2003)	0	0.0223	0.017
DAV08	$[SO_4^{2-}]$, $[NO_3^-]$, $[NH_4^+]$, RH, T	$\boldsymbol{\gamma = x_1 \times \gamma_1^* + x_2 \times \gamma_2^* + x_3 \times \gamma_3^*}$ where, $\lambda_1=-4.10612+0.02386\times RH-0.23771\times \max((T-291),0)$ $\gamma_1=1/(1+e^{-\lambda_1})$ $\gamma_1^*=\min(\gamma_1, 0.08585)$ $\lambda_2=(-4.10612-0.80570)+0.02386\times RH+(-0.23771+0.10225)\times \max((T-291),0)$ $\gamma_2=1/(1+e^{-\lambda_2})$ $\gamma_2^*=\min(\gamma_2, 0.053)$ $\lambda_3=-8.10774+0.04902\times RH$ $\gamma_3=1/(1+e^{-\lambda_3})$ $\gamma_3^*=\min(\gamma_3, 0.0154)$ $x_3=[NO_3^-]/([NO_3^-]+[SO_4^{2-}])$ $x_2=\max(0, \min(1-x_3, [NH_4^+]/([NO_3^-]+[SO_4^{2-}])-1))$ $x_1=1-x_2-x_3$	(Davis et al., 2008)	0.02	00317	0.034

Parameterization name	Factors considered	Parameterization	Reference	R^2	RMSE	Median
		(1=NH_4HSO_4, 2=$(NH_4)_2SO_4$, 3=NH_4NO_3)				
BT09	ALWC, $[NO_3^-]$, $[Cl^-]$, V_a, S_a	$\gamma = \frac{4}{c}\frac{V_a}{S_a}K_H k'_{2f}\left(1 - \frac{1}{\left(\frac{k_3[H_2O]}{k_{2b}[NO_3^-]}\right) + 1 + \left(\frac{k_4[Cl^-]}{k_{2b}[NO_3^-]}\right)}\right)$ where, K_H=51, Henry's Law Coefficient (Fried et al., 1994) $k'_{2f}=\beta - \beta_e^{(-\delta[H_2O])}$ $\beta=1.15\times10^6$ (s^{-1}) $\delta=0.13$ (M^{-1}) $\frac{k_3}{k_{2b}}=0.06$ $\frac{k_4}{k_{2b}}=29$	(Bertram and Thornton, 2009)	0.06	0.0228	0.034
BT09 w/o Cl	ALWC, $[NO_3^-]$, V_a, S_a	$\gamma = \frac{4}{c}\frac{V_a}{S_a}K_H k'_{2f}\left(1 - \frac{1}{\left(\frac{k_3[H_2O]}{k_{2b}[NO_3^-]}\right) + 1}\right)$ parameters are same as BT09.	(Bertram and Thornton, 2009)	0.07	0.0202	0.020
GRI09	ALWC, $[NO_3^-]$, V_a, S_a	$\gamma = \frac{4}{c}\frac{V_a}{S_a}K_H k'_{2f}\left(1 - \frac{1}{\left(\frac{k_3[H_2O]}{k_{2b}[NO_3^-]}\right) + 1}\right)$	(Griffiths et al., 2009)	0.06	0.0533	0.063

Parameterization name	Factors considered	Parameterization	Reference	R^2	RMSE	Median
		Where, K_H=51 $\frac{k_3}{k_{2b}}$=1/30 k'_{2f}=5×10^6				
YU20	ALWC, [NO_3^-], [Cl^-], V_a, S_a	$\gamma = \frac{4}{c}\frac{V_a}{S_a} K_H k'_{2f} \left(1 - \frac{1}{\left(\frac{k_3[\mathrm{H_2O}]}{k_{2b}[\mathrm{NO_3}^-]}\right) + 1 + \left(\frac{k_4[Cl^-]}{k_{2b}[\mathrm{NO_3}^-]}\right)} \right)$ where, K_H=51 k'_{2f}=[H_2O]×3×10^4 $\frac{k_3}{k_{2b}}$=0.033 $\frac{k_4}{k_{2b}}$=3.4	(Yu et al., 2020)	0.09	0.02	0.019
EJ05	Mass fraction of aerosol sulfate and organic, RH,	**γ=mass SO_4^{2-}/dry mass×γ_1+mass organic/dry mass×γ_2** where, γ_1=α×10$^\beta$ α=2.79×10^{-4}+1.3×10^{-4}×RH−3.43×10^{-6}×RH^2+7.52×10^{-8} ×RH^3	(Evans and Jacob, 2005)	0	0.0228	0.019

Parameterization name	Factors considered	Parameterization	Reference	R^2	RMSE	Median
	T	$\beta=4\times10^{-2}\times(T-294)$, ($T\geq282K$) $\beta=-0.48$, ($T<282K$) $\gamma_2=RH\times5.2\times10^{-4}$, ($RH<57\%$) $\gamma_2=0.03$, ($RH\geq57\%$)				
BT09+Rie09	ALWC, $[NO_3^-]$, $[Cl^-]$, V_a, S_a, organic coating	$\frac{1}{\gamma}=\frac{1}{\gamma_{core}}+\frac{1}{\gamma_{org.coat}}$ where, γ_{core}=BT09 $\gamma_{org.coat}=\frac{4RTD_{org}H_{org}R_c}{clR_p}$ R, gas constant ($atm\cdot m^3/mol\cdot K$) T, temperature (K) $D_{org}H_{org}=\varepsilon D_{aq}H_{aq}$ $\varepsilon=0.03$ H_{aq}=5000, Henry's Law Coefficient in aqueous core ($mol\ m^{-3}\ atm^{-1}$) $D_{aq}=1\times10^{-9}$, N_2O_5 Liquid Diffusion Coefficient ($m^2\ s^{-1}$) R_p, median particle total radius, (m) $R_c=R_p-l$, particle core radius (m) $l=R_p\times(1-\beta^{1/3})$, organic coating thickness (m) $\beta=V_{inorganic}/(V_{organic}+V_{inorganic})$	(Bertram and Thornton, 2009;Anttila et al., 2006;Riemer et al., 2009)	0.03	0.0278	0.012
BT09+Rie09(wG14)	ALWC, $[NO_3^-]$, $[Cl^-]$,	$\frac{1}{\gamma}=\frac{1}{\gamma_{core}}+\frac{1}{\gamma_{org.coat}}$	(Gaston et al., 2014)	0.07 (O/C=0.8);	0.0201 (O/C=0.8);	0.019 (O/C=0.8);

Parameterization name	Factors considered	Parameterization	Reference	R^2	RMSE	Median
	V_a, S_a, organic coating, O/C, RH	same as BT09+Rie09 except, ε=0.06, (RH⩽30% and O/C⩾0.7) ε=0.008, (RH⩽30% and O/C⩽0.7) ε=0.3, (30%⩽RH⩽70% and O/C⩾0.7) ε=0.05, (30%⩽RH⩽70% and O/C⩽0.7) ε=1.0, (70%⩽RH and O/C⩾0.7) ε=0.8, (70%⩽RH and O/C⩽0.7)		0.07 (O/C=0.5)	0.0248 (O/C=0.5)	0.006 (O/C=0.5)
MD18	ALWC, $[NO_3^-]$, $[Cl^-]$, V_a, S_a, organic coating, O/C, RH	$\frac{1}{\gamma}=\frac{1}{\gamma_{core}}+\frac{1}{\gamma_{org.coat}}$ same as BT09+Rie09 except, γ_{core}=BT09 w/o Cl k'_{2f}=$[H_2O]\times2.14\times10^5$ $\frac{k_3}{k_{2b}}$=0.04 ε=0.15×O/C+0.0016×RH	(McDuffie et al., 2018)	0.05 (O/C=0.8); 0.04 (O/C=0.5)	0.0205 (O/C=0.8); 0.0208 (O/C=0.5)	0.022 (O/C=0.8); 0.018 (O/C=0.5)

References:

Aldener, M., Brown, S. S., Stark, H., Williams, E. J., Lerner, B. M., Kuster, W. C., Goldan, P. D., Quinn, P. K., Bates, T. S., Fehsenfeld, F. C., and Ravishankara, A. R.: Reactivity and loss mechanisms of NO_3 and N_2O_5 in a polluted marine environment: Results from in situ measurements during New England Air Quality Study 2002, Journal of Geophysical Research-Atmospheres, 111, 10.1029/2006jd007252, 2006.

Anttila, T., Kiendler-Scharr, A., Tillmann, R., and Mentel, T. F.: On the reactive uptake of gaseous compounds by organic-coated aqueous aerosols: Theoretical analysis and application to the heterogeneous hydrolysis of N_2O_5, Journal of Physical Chemistry A, 110, 10435-10443, 10.1021/jp062403c, 2006.

Bertram, T. H., and Thornton, J. A.: Toward a general parameterization of N_2O_5 reactivity on aqueous particles: the competing effects of particle liquid water, nitrate and chloride, Atmospheric Chemistry and Physics, 9, 8351-8363, 10.5194/acp-9-8351-2009, 2009.

Bertram, T. H., Thornton, J. A., and Riedel, T. P.: An experimental technique for the direct measurement of N_2O_5 reactivity on ambient particles, Atmospheric Measurement Techniques, 2, 231-242, 10.5194/amt-2-231-2009, 2009.

Brown, S. S., Dibb, J. E., Stark, H., Aldener, M., Vozella, M., Whitlow, S., Williams, E. J., Lerner, B. M., Jakoubek, R., Middlebrook, A. M., DeGouw, J. A., Warneke, C., Goldan, P. D., Kuster, W. C., Angevine, W. M., Sueper, D. T., Quinn, P. K., Bates, T. S., Meagher, J. F., Fehsenfeld, F. C., and Ravishankara, A. R.: Nighttime removal of NOx in the summer marine boundary layer, Geophysical Research Letters, 31, 10.1029/2004gl019412, 2004.

Brown, S. S., Ryerson, T. B., Wollny, A. G., Brock, C. A., Peltier, R., Sullivan, A. P., Weber, R. J., Dube, W. P., Trainer, M., Meagher, J. F., Fehsenfeld, F. C., and Ravishankara, A. R.: Variability in nocturnal nitrogen oxide processing and its role in regional air quality, Science, 311, 67-70, 10.1126/science.1120120, 2006.

Brown, S. S., Dube, W. P., Fuchs, H., Ryerson, T. B., Wollny, A. G., Brock, C. A., Bahreini, R., Middlebrook, A. M., Neuman, J. A., Atlas, E., Roberts, J. M., Osthoff, H. D., Trainer, M., Fehsenfeld, F. C., and Ravishankara, A. R.: Reactive uptake coefficients for N_2O_5 determined from aircraft measurements during the Second Texas Air Quality Study: Comparison to current model parameterizations, Journal of Geophysical Research-Atmospheres, 114, 10.1029/2008jd011679, 2009.

Brown, S. S., Dube, W. P., Tham, Y. J., Zha, Q. Z., Xue, L. K., Poon, S., Wang, Z., Blake, D. R., Tsui, W., Parrish, D. D., and Wang, T.: Nighttime chemistry at a high altitude site above Hong Kong, Journal of Geophysical Research-Atmospheres, 121, 2457-2475, 10.1002/2015jd024566, 2016.

Brown, S. S., An, H., Lee, M., Park, J. H., Lee, S. D., Fibiger, D. L., McDuffie, E. E., Dube, W. P., Wagner, N. L., and Min, K. E.: Cavity enhanced spectroscopy for measurement of nitrogen oxides in the Anthropocene: results from the Seoul tower during MAPS 2015, Faraday Discussions, 200, 529-557, 10.1039/c7fd00001d, 2017.

Chang, W. L., Brown, S. S., Stutz, J., Middlebrook, A. M., Bahreini, R., Wagner, N. L., Dube, W. P., Pollack, I. B., Ryerson, T. B., and Riemer, N.: Evaluating N_2O_5 heterogeneous hydrolysis parameterizations for CalNex 2010, Journal of Geophysical Research-Atmospheres, 121, 5051-5070, 10.1002/2015jd024737, 2016.

Chen, X., Wang, H., Zhai, T., Li, C., and Lu, K.: Direct measurement of N_2O_5 heterogeneous uptake coefficients on ambient aerosols via an aerosol flow tube system: design, characterizationand performance, Atmospheric Measurement Techniques, 15, 7019-7037, 10.5194/amt-15-7019-2022, 2022.

Chen, X. R., Wang, H. C., Lu, K. D., Li, C. M., Zhai, T. Y., Tan, Z. F., Ma, X. F., Yang, X. P., Liu, Y. H., Chen, S. Y., Dong, H. B., Li, X., Wu, Z. J., Hu, M., Zeng, L. M., and Zhang, Y. H.: Field Determination of Nitrate Formation Pathway in Winter Beijing, Environmental Science & Technology, 54, 9243-9253, 10.1021/acs.est.0c00972, 2020.

Crowley, J. N., Thieser, J., Tang, M. J., Schuster, G., Bozem, H., Beygi, Z. H., Fischer, H., Diesch, J. M., Drewnick, F., Borrmann, S., Song, W., Yassaa, N., Williams, J., Pohler, D., Platt, U., and Lelieveld, J.: Variable lifetimes and loss mechanisms for NO_3 and N_2O_5 during the DOMINO campaign: contrasts between marine, urban and continental air, Atmospheric Chemistry and Physics, 11, 10853-10870, 10.5194/acp-11-10853-2011, 2011.

Davis, J. M., Bhave, P. V., and Foley, K. M.: Parameterization of N_2O_5 reaction probabilities on the surface of particles containing ammonium, sulfate, and nitrate, Atmospheric Chemistry and Physics, 8, 5295-5311, 10.5194/acp-8-5295-2008, 2008.

Evans, M. J., and Jacob, D. J.: Impact of new laboratory studies of N_2O_5 hydrolysis on global model budgets of tropospheric nitrogen oxides, ozone, and OH, Geophysical Research Letters, 32, 10.1029/2005gl022469, 2005.

Fried, A., Henry, B. E., Calvert, J. G., and Mozurkewich, M.: The reaction probability of n_2o_5 with sulfuric-acid aerosols at stratospheric temperatures and compositions, Journal of Geophysical Research-Atmospheres, 99, 3517-3532, 10.1029/93jd01907, 1994.

Gaston, C. J., Thornton, J. A., and Ng, N. L.: Reactive uptake of N_2O_5 to internally mixed inorganic and organic particles: the role of organic carbon oxidation state and inferred organic phase separations, Atmospheric Chemistry and Physics, 14, 5693-5707, 10.5194/acp-14-5693-2014, 2014.

Griffiths, P. T., Badger, C. L., Cox, R. A., Folkers, M., Henk, H. H., and Mentel, T. F.: Reactive Uptake of N_2O_5 by Aerosols Containing Dicarboxylic Acids. Effect of Particle Phase, Composition, and Nitrate Content, Journal of Physical Chemistry A, 113, 5082-5090, 10.1021/jp8096814, 2009.

Li, Z. Y., Xie, P. H., Hu, R. Z., Wang, D., Jin, H. W., Chen, H., Lin, C., and Liu, W. Q.: Observations of N_2O_5 and NO_3 at a suburban environment in Yangtze river delta in China: Estimating heterogeneous N_2O_5 uptake coefficients, Journal of Environmental Sciences, 95, 248-255, 10.1016/j.jes.2020.04.041, 2020.

Lu, X., Qin, M., Xie, P. H., Duan, J., Fang, W., and Liu, W. Q.: Observation of ambient NO_3 radicals by LP-DOAS at a rural site in North China Plain, Science of the

Total Environment, 804, 10.1016/j.scitotenv.2021.149680, 2022.

McDuffie, E. E., Fibiger, D. L., Dube, W. P., Lopez-Hilfiker, F., Lee, B. H., Thornton, J. A., Shah, V., Jaegle, L., Guo, H. Y., Weber, R. J., Reeves, J. M., Weinheimer, A. J., Schroder, J. C., Campuzano-Jost, P., Jimenez, J. L., Dibb, J. E., Veres, P., Ebben, C., Sparks, T. L., Wooldridge, P. J., Cohen, R. C., Hornbrook, R. S., Apel, E. C., Campos, T., Hall, S. R., Ullmann, K., and Brown, S. S.: Heterogeneous N_2O_5 Uptake During Winter: Aircraft Measurements During the 2015 WINTER Campaign and Critical Evaluation of Current Parameterizations, Journal of Geophysical Research-Atmospheres, 123, 4345-4372, 10.1002/2018jd028336, 2018.

McDuffie, E. E., Womack, C. C., Fibiger, D. L., Dube, W. P., Franchin, A., Middlebrook, A. M., Goldberger, L., Lee, B., Thornton, J. A., Moravek, A., Murphy, J. G., Baasandorj, M., and Brown, S. S.: On the contribution of nocturnal heterogeneous reactive nitrogen chemistry to particulate matter formation during wintertime pollution events in Northern Utah, Atmospheric Chemistry and Physics, 19, 9287-9308, 10.5194/acp-19-9287-2019, 2019.

Morgan, W. T., Ouyang, B., Allan, J. D., Aruffo, E., Di Carlo, P., Kennedy, O. J., Lowe, D., Flynn, M. J., Rosenberg, P. D., Williams, P. I., Jones, R., McFiggans, G. B., and Coe, H.: Influence of aerosol chemical composition on N_2O_5 uptake: airborne regional measurements in northwestern Europe, Atmospheric Chemistry and Physics, 15, 973-990, 10.5194/acp-15-973-2015, 2015.

Niu, Y. B., Zhu, B., He, L. Y., Wang, Z., Lin, X. Y., Tang, M. X., and Huang, X. F.: Fast Nocturnal Heterogeneous Chemistry in a Coastal Background Atmosphere and Its Implications for Daytime Photochemistry, Journal of Geophysical Research-Atmospheres, 127, 10.1029/2022jd036716, 2022.

Osthoff, H. D., Odame-Ankrah, C. A., Taha, Y. M., Tokarek, T. W., Schiller, C. L., Haga, D., Jones, K., and Vingarzan, R.: Low levels of nitryl chloride at ground level: nocturnal nitrogen oxides in the Lower Fraser Valley of British Columbia, Atmospheric Chemistry and Physics, 18, 6293-6315, 10.5194/acp-18-6293-2018, 2018.

Phillips, G. J., Thieser, J., Tang, M. J., Sobanski, N., Schuster, G., Fachinger, J., Drewnick, F., Borrmann, S., Bingemer, H., Lelieveld, J., and Crowley, J. N.: Estimating N_2O_5 uptake coefficients using ambient measurements of NO_3, N_2O_5, $ClNO_2$ and particle-phase nitrate, Atmospheric Chemistry and Physics, 16, 13231-13249, 10.5194/acp-16-13231-2016, 2016.

Riedel, T. P., Bertram, T. H., Ryder, O. S., Liu, S., Day, D. A., Russell, L. M., Gaston, C. J., Prather, K. A., and Thornton, J. A.: Direct N_2O_5 reactivity measurements at a polluted coastal site, Atmospheric Chemistry and Physics, 12, 2959-2968, 10.5194/acp-12-2959-2012, 2012.

Riemer, N., Vogel, H., Vogel, B., Schell, B., Ackermann, I., Kessler, C., and Hass, H.: Impact of the heterogeneous hydrolysis of N_2O_5 on chemistry and nitrate aerosol formation in the lower troposphere under photosmog conditions, Journal of Geophysical Research-Atmospheres, 108, 10.1029/2002jd002436, 2003.

Riemer, N., Vogel, H., Vogel, B., Anttila, T., Kiendler-Scharr, A., and Mentel, T.

F.: Relative importance of organic coatings for the heterogeneous hydrolysis of N_2O_5 during summer in Europe, Journal of Geophysical Research-Atmospheres, 114, 10.1029/2008jd011369, 2009.

Tham, Y. J., Wang, Z., Li, Q. Y., Yun, H., Wang, W. H., Wang, X. F., Xue, L. K., Lu, K. D., Ma, N., Bohn, B., Li, X., Kecorius, S., Gross, J., Shao, M., Wiedensohler, A., Zhang, Y. H., and Wang, T.: Significant concentrations of nitryl chloride sustained in the morning: investigations of the causes and impacts on ozone production in a polluted region of northern China, Atmospheric Chemistry and Physics, 16, 14959-14977, 10.5194/acp-16-14959-2016, 2016.

Tham, Y. J., Wang, Z., Li, Q. Y., Wang, W. H., Wang, X. F., Lu, K. D., Ma, N., Yan, C., Kecorius, S., Wiedensohler, A., Zhang, Y. H., and Wang, T.: Heterogeneous N_2O_5 uptake coefficient and production yield of $ClNO_2$ in polluted northern China: roles of aerosol water content and chemical composition, Atmospheric Chemistry and Physics, 18, 13155-13171, 10.5194/acp-18-13155-2018, 2018.

Wagner, N. L., Riedel, T. P., Young, C. J., Bahreini, R., Brock, C. A., Dube, W. P., Kim, S., Middlebrook, A. M., Ozturk, F., Roberts, J. M., Russo, R., Sive, B., Swarthout, R., Thornton, J. A., VandenBoer, T. C., Zhou, Y., and Brown, S. S.: N_2O_5 uptake coefficients and nocturnal NO_2 removal rates determined from ambient wintertime measurements, Journal of Geophysical Research-Atmospheres, 118, 9331-9350, 10.1002/jgrd.50653, 2013.

Wang, H. C., Lu, K. D., Chen, X. R., Zhu, Q. D., Chen, Q., Guo, S., Jiang, M. Q., Li, X., Shang, D. J., Tan, Z. F., Wu, Y. S., Wu, Z. J., Zou, Q., Zheng, Y., Zeng, L. M., Zhu, T., Hu, M., and Zhang, Y. H.: High N_2O_5 Concentrations Observed in Urban Beijing: Implications of a Large Nitrate Formation Pathway, Environmental Science & Technology Letters, 4, 416-420, 10.1021/acs.estlett.7b00341, 2017a.

Wang, H. C., Lu, K. D., Guo, S., Wu, Z. J., Shang, D. J., Tan, Z. F., Wang, Y. J., Le Breton, M., Lou, S. R., Tang, M. J., Wu, Y. S., Zhu, W. F., Zheng, J., Zeng, L. M., Hallquist, M., Hu, M., and Zhang, Y. H.: Efficient N_2O_5 uptake and NO_3 oxidation in the outflow of urban Beijing, Atmospheric Chemistry and Physics, 18, 9705-9721, 10.5194/acp-18-9705-2018, 2018.

Wang, H. C., Chen, X. R., Lu, K. D., Hu, R. Z., Li, Z. Y., Wang, H. L., Ma, X. F., Yang, X. P., Chen, S. Y., Dong, H. B., Liu, Y., Fang, X., Zeng, L. M., Hu, M., and Zhang, Y. H.: NO_3 and N_2O_5 chemistry at a suburban site during the EXPLORE-YRD campaign in 2018, Atmospheric Environment, 224, 10.1016/j.atmosenv.2019.117180, 2020a.

Wang, H. C., Chen, X. R., Lu, K. D., Tan, Z. F., Ma, X. F., Wu, Z. J., Li, X., Liu, Y. H., Shang, D. J., Wu, Y. S., Zeng, L. M., Hu, M., Schmitt, S., Kiendler-Scharr, A., Wahner, A., and Zhang, Y. H.: Wintertime N_2O_5 uptake coefficients over the North China Plain, Science Bulletin, 65, 765-774, 10.1016/j.scib.2020.02.006, 2020b.

Wang, H. C., Yuan, B., Zheng, E., Zhang, X. X., Wang, J., Lu, K. D., Ye, C. S., Yang, L., Huang, S., Hu, W. W., Yang, S. X., Peng, Y. W., Qi, J. P., Wang, S. H., He, X. J., Chen, Y. B., Li, T. G., Wang, W. J., Huangfu, Y. B., Li, X. B., Cai, M. F., Wang, X.

M., and Shao, M.: Formation and impacts of nitryl chloride in Pearl River Delta, Atmospheric Chemistry and Physics, 22, 14837-14858, 10.5194/acp-22-14837-2022, 2022.

Wang, J., Wang, H. C., Tham, Y. J., Ming, L. L., Zheng, Z. L., Fang, G. Z., Sun, C. Z., Ling, Z. H., Zhao, J., and Fan, S. J.: Measurement report: Atmospheric nitrate radical chemistry in the South China Sea influenced by the urban outflow of the Pearl River Delta, Atmospheric Chemistry and Physics, 24, 977-992, 10.5194/acp-24-977-2024, 2024.

Wang, S. S., Shi, C. Z., Zhou, B., Zhao, H., Wang, Z. R., Yang, S. N., and Chen, L. M.: Observation of NO₃ radicals over Shanghai, China, Atmospheric Environment, 70, 401-409, 10.1016/j.atmosenv.2013.01.022, 2013.

Wang, X. F., Wang, H., Xue, L. K., Wang, T., Wang, L. W., Gu, R. R., Wang, W. H., Tham, Y. J., Wang, Z., Yang, L. X., Chen, J. M., and Wang, W. X.: Observations of N_2O_5 and $ClNO_2$ at a polluted urban surface site in North China: High N_2O_5 uptake coefficients and low $ClNO_2$ product yields, Atmospheric Environment, 156, 125-134, 10.1016/j.atmosenv.2017.02.035, 2017b.

Wang, Z., Wang, W. H., Tham, Y. J., Li, Q. Y., Wang, H., Wen, L., Wang, X. F., and Wang, T.: Fast heterogeneous N_2O_5 uptake and $ClNO_2$ production in power plant and industrial plumes observed in the nocturnal residual layer over the North China Plain, Atmospheric Chemistry and Physics, 17, 12361-12378, 10.5194/acp-17-12361-2017, 2017c.

Wood, E. C., Bertram, T. H., Wooldridge, P. J., and Cohen, R. C.: Measurements of N₂O₅, NO₂, and O₃ east of the San Francisco Bay, Atmospheric Chemistry and Physics, 5, 483-491, 10.5194/acp-5-483-2005, 2005.

Xia, M., Peng, X., Wang, W. H., Yu, C. A., Wang, Z., Tham, Y. J., Chen, J. M., Chen, H., Mu, Y. J., Zhang, C. L., Liu, P. F., Xue, L. K., Wang, X. F., Gao, J., Li, H., and Wang, T.: Winter $ClNO_2$ formation in the region of fresh anthropogenic emissions: seasonal variability and insights into daytime peaks in northern China, Atmospheric Chemistry and Physics, 21, 15985-16000, 10.5194/acp-21-15985-2021, 2021.

Yan, C., Tham, Y. J., Zha, Q., Wang, X., Xue, L., Dai, J., Wang, Z., and Wang, T.: Fast heterogeneous loss of N_2O_5 leads to significant nighttime NOx removal and nitrate aerosol formation at a coastal background environment of southern China, Science of the Total Environment, 677, 637-647, 10.1016/j.scitotenv.2019.04.389, 2019.

Yu, C., Wang, Z., Xia, M., Fu, X., Wang, W. H., Tham, Y. J., Chen, T. S., Zheng, P. G., Li, H. Y., Shan, Y., Wang, X. F., Xue, L. K., Zhou, Y., Yue, D. L., Ou, Y. B., Gao, J., Lu, K. D., Brown, S. S., Zhang, Y. H., and Wang, T.: Heterogeneous N_2O_5 reactions on atmospheric aerosols at four Chinese sites: improving model representation of uptake parameters, Atmospheric Chemistry and Physics, 20, 4367-4378, 10.5194/acp-20-4367-2020, 2020.

Yun, H., Wang, T., Wang, W. H., Tham, Y. J., Li, Q. Y., Wang, Z., and Poon, S. C. N.: Nighttime NOx loss and $ClNO_2$ formation in the residual layer of a polluted region:

Insights from field measurements and an iterative box model, Science of the Total Environment, 622, 727-734, 10.1016/j.scitotenv.2017.11.352, 2018.

Zhai, T. Y., Lu, K. D., Wang, H. C., Lou, S. R., Chen, X. R., Hu, R. Z., and Zhang, Y. H.: Elucidate the formation mechanism of particulate nitrate based on direct radical observations in the Yangtze River Delta summer 2019, Atmospheric Chemistry and Physics, 23, 2379-2391, 10.5194/acp-23-2379-2023, 2023.